Heterogeneous Chemistry of HO_2NO_2 in Liquid Sulfuric Acid

Renyi Zhang, Ming-Taun Leu,* and Leon F. Keyser

Earth and Space Sciences Division, Jet Propulsion Laboratory, California Institute of Technology, Pasadena, California 91109

Received: October 24, 1996; In Final Form: March 10, 1997[⊗]

The interaction of HO_2NO_2 (peroxynitric acid, PNA) vapor with liquid sulfuric acid was investigated for acid contents ranging from 53 to 74 wt % and at temperatures between 205 and 230 K, using a fast-flow reactor coupled to a chemical ionization mass spectrometer. PNA was observed to be physically taken up by liquid sulfuric acid, without undergoing irreversible aqueous-phase reactions. From the time-dependent uptake, the quantity $H^*\sqrt{D_l}$ (that is, the product of the effective Henry's law solubility constant and the square root of the liquid-phase diffusion coefficient) was obtained. The effective Henry's law solubility constant H^* of PNA in liquid sulfuric acid was derived by estimating the liquid-phase diffusion coefficient based on a cubic cell model. In general, the solubility was found to increase with decreasing acid content and decreasing temperature. The heterogeneous reaction between PNA and HCl in liquid sulfuric acid was also examined and was found to be very slow ($\gamma < 1 \times 10^{-4}$). The measured solubility reveals that PNA should exist predominately in the gas phase under conditions characteristic of the middle or lower latitude stratosphere. For winter polar stratospheric conditions, however, incorporation of PNA into sulfate aerosols may lead to redistribution of PNA from the gas to condensed phases, potentially affecting stratospheric HO_x and NO_x concentrations.

Introduction

Heterogeneous reactions occurring on stratospheric sulfate aerosols have been known to enhance ozone destruction,[1,2] primarily by converting relatively inactive chlorine reservoir species into reactive forms (i.e., $ClONO_2$ and HCl into Cl_2 and HOCl) that are rapidly photolyzed to yield atomic chlorine and catalytically destroy ozone. Hydrolysis of N_2O_5 on sulfate aerosols is also believed to reduce the stratospheric NO_x concentration and consequently result in increases in the abundances of ClO and OH. Under unperturbed stratospheric conditions, the sulfate aerosols are believed to consist of aqueous sulfuric acid of 40−80 wt %, with a mean diameter of about 0.1 μm and a number density from 1 to 10 cm^{-3}.[3] Although much effort has been made to study heterogeneous processes involving N_2O_5, $ClONO_2$, HCl, and HOCl on sulfate aerosols,[1,2] which promote the release of active chlorine and affect the NO_x budget, little is known about heterogeneous chemistry involving other nitrogen-containing acids and oxides in liquid sulfuric acid. For example, peroxynitric acid (PNA) may have potential importance in aqueous atmospheric chemistry in at least two ways: incorporation of PNA into sulfate aerosols may alter the aerosol composition and repartition PNA from the gas to condensed phases (thus affecting the HO_x and NO_x budgets); HO_2NO_2 may also engage in heterogeneous reactions, such as that with HCl to form HOCl or decomposition to produce HONO.

In the stratosphere HO_2NO_2 is present at concentrations of a few tenths of part per billion by volume (ppbv) and is formed mainly by the reaction of HO_2 with NO_2:[4,5]

$$HO_2 + NO_2 + M \rightarrow HO_2NO_2 + M \qquad (1)$$

The fate of gaseous PNA is governed by unimolecular decomposition as well as photodissociation and bimolecular reaction with OH. Under stratospheric conditions, PNA is photolyzed with a lifetime of about a few days.[6,7] Photolysis of PNA at wavelengths greater than 290 nm yields primarily HO_2 and NO_2, along with minor OH and NO_3.[8] The bimolecular reaction of PNA with OH is very efficient, with a rate coefficient of 4.6×10^{-12} cm^3 s^{-1}.[1] Other likely homogeneous reaction pathways include the reactions of PNA with O, H, and HCl, although these reactions are several orders of magnitude slower than that between PNA and OH.[1]

In contrast, the role of PNA in heterogeneous atmospheric chemistry is less certain. In aqueous solutions HO_2NO_2 undergoes unimolecular decomposition producing HONO and O_2:[9,10]

$$HO_2NO_2 \rightarrow HONO + O_2 \qquad (2)$$

The decomposition rate ($\sim 7 \times 10^{-4}$ s^{-1}) measured in previous studies, however, suggests that this reaction may be too slow to be of atmospheric importance, unless the solubility of PNA is extremely large. In another recent study it has been postulated that heterogeneous decomposition of PNA may be responsible for significant production of nitrous acid (HONO) observed in an environmental chamber experiment.[11] The same reaction mechanism has also been invoked to explain the observed anomalous OH and HO_2 concentrations shortly after sunrise in stratospheric field measurements:[12,13] this process occurring on sulfate aerosols may redistribute HO_x at large solar zenith angles. Recently, Li et al.[14] have investigated PNA uptake on water ice. These authors reported a sticking coefficient of 0.15 for PNA on ice at about 200 K and found no reaction products in their experiments. The uptake coefficient of PNA in a 96 wt % sulfuric acid was also investigated by Baldwin and Golden at room temperature,[15] yielding a value of 2.7×10^{-5}. Clearly, more laboratory studies are needed in order to elucidate the interaction of PNA with sulfate aerosols in the stratosphere.

In this paper we present laboratory measurements of critical parameters needed to quantify the interaction of PNA vapor with liquid sulfuric acid. These include the uptake coefficient and solubility of PNA in liquid H_2SO_4. From the time-

* To whom correspondence should be addressed.

[⊗] Abstract published in *Advance ACS Abstracts,* April 15, 1997.

S1089-5639(96)03321-X CCC: $14.00

dependent uptake, the product of the effective Henry's law solubility constant and the square root of the liquid-phase diffusion coefficient, $H^*\sqrt{D_l}$, was measured. The effective Henry's law solubility constant, H^*, was then deduced by estimating the liquid-phase diffusion coefficient based on a cubic cell model. Potential heterogeneous reaction involving HO_2NO_2 with HCl on liquid sulfuric acid was also examined. Finally, stratospheric implications of the present data are discussed.

Experimental Method

Uptake measurements were conducted in a fast-flow reactor in conjunction with chemical ionization mass spectrometry (CIMS) detection. Detailed descriptions of the experimental apparatus and procedures have been given elsewhere,[16−18] and only a brief overview is presented here along with features pertinent to this work.

The flow reactor of inner diameter 2.8 cm was horizontally mounted and temperature regulated. Liquid H_2SO_4 films were prepared by totally covering the inside wall of the flow tube with sulfuric acid solutions. At low temperatures (<220 K) the solutions were sufficiently viscous to produce essentially a static film which lasted over the time scale of the experiments. The thickness of the films was estimated to be about 0.1 mm based on the amount of acid solution used and the geometric area covered, but in some cases it may be thinner than the estimated. Composition of the liquid H_2SO_4 film was governed by the temperature and H_2O partial pressure in the flow tube: once exposed to H_2O vapor, the sulfuric acid film took up H_2O and became more dilute until equilibrium was reached. H_2O vapor was admitted into the flow tube with the main He carrier gas; its partial pressure was estimated by passing a known flow of He carrier gas through a H_2O reservoir at room temperature. It was controlled by diluting the humidified He flow (assuming 100% relative humidity) with a dry He flow. In addition, we measured $ClONO_2$ hydrolysis in the liquid H_2SO_4/H_2O film and obtained its composition, on the basis of our earlier data of the reaction probabilities in this binary system,[16] to validate the above method. The estimated uncertainty in determining the H_2O partial pressure was about ±25%. To deduce the H_2SO_4 content of the liquid film, we used the temperature and H_2O partial pressure to obtain the H_2SO_4 wt %, according to the vapor pressure data of Zeleznik[19] and Zhang et al.[20] The error limit of estimating the H_2SO_4 content of the films using this method was about 1−2 wt %, considering uncertainties associated with the measurements of the temperature and water vapor pressure. In addition, some uptake measurements of PNA were performed by directly preparing liquid sulfuric acid of known compositions on the inner walls of the flow reactor. The acid compositions were determined by weighing a known volume of the solutions and using H_2SO_4 specific gravity, with an estimated uncertainty of about ±0.5 wt % in the acid content. For these experiments, water vapor was also added to the flow reactor in order to prevent H_2O evaporation from the liquid film and subsequent change in the acid composition. The results obtained using these two approaches were found to be consistent within the experimental uncertainties.

PNA was synthesized by slowly adding ∼1 g of NO_2BF_4 (Aldrich) to ∼5 mL of 93 wt % H_2O_2 which was chilled (at 273 K) and vigorously stirred, according to the method described by Kenley et al.[9] The solution containing PNA was then transferred to a bubbler maintained at 273 K. The purity of PNA samples was checked by both infrared spectroscopy and mass spectrometry, with NO_2, HNO_3, H_2O_2, and H_2O being the major impurities. Generally, the amounts of HNO_3 and NO_2 in the PNA sample were reduced significantly after bubbling the solution for more than 10 min. A jacketed Pyrex injector (1.0-cm o.d.), kept warm by circulating a room-temperature solution of ethylene glycol in water, was used to deliver PNA to the flow reactor. Gaseous PNA was added to the flow tube along with a small He flow (0.1−10.0 $cm^3\ min^{-1}$ at STP) and further diluted in the main He flow (310 $cm^3\ min^{-1}$ at STP) before contacting the liquid acid surface. To reduce the H_2O_2 and H_2O impurities, the PNA flow was circulated through a cold trap at temperatures between 230 and 240 K, prior to entering the flow tube. A three-way switching valve was designed to quickly change the PNA flow either downstream or upstream (i.e., to expose or bypass the PNA gas to sulfuric acid), with a delay time less than 50 ms. Since the position of the PNA injector remained unchanged during an uptake experiment, the uncertainty in determining the area of the exposed liquid surface should be negligible. Typically, the flow tube was operated at a pressure of about 0.40 Torr, with an average flow velocity ranging from 1700 to 2000 cm s^{-1}.

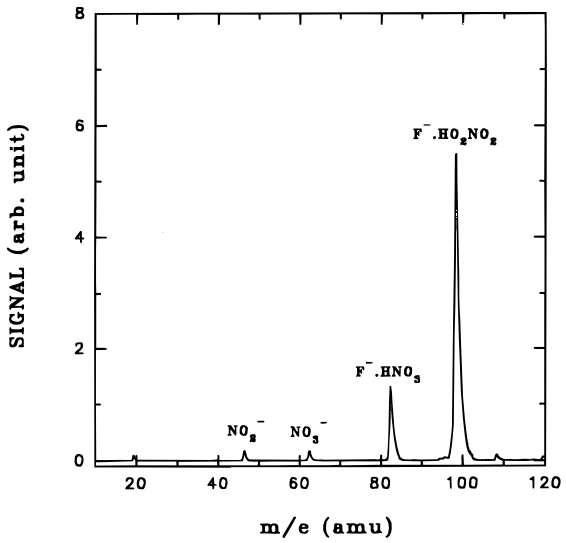

Figure 1. Mass spectrum of SF_6^- reaction with the effluent from a PNA bubbler. $F^-\cdot HO_2NO_2$ (m/e = 98) is formed via a fluoride ion transfer from SF_6^- to HO_2NO_2. Impurities in the PNA sample are recognized primarily as NO_2 (NO_2^-, m/e = 46) and HNO_3 ($F^-\cdot HNO_3$, m/e = 82). Other small, yet distinguishable peaks are due to F^- (m/e = 19), NO_3^- (m/e = 62), and SF_4^- (m/e = 108).

In most experiments, HO_2NO_2 was detected in the CIMS as $F^-\cdot HO_2NO_2$, produced by a fluoride ion transfer with SF_6^-:

$$SF_6^- + HO_2NO_2 \rightarrow F^-\cdot HO_2NO_2 + SF_5 \qquad (3)$$

A typical mass spectrum of SF_6^- reaction with the effluent from the PNA bubbler is displayed in Figure 1, showing the characteristic HO_2NO_2 peak ($F^-\cdot HO_2NO_2$, m/e = 98) along with the impurity peaks due to NO_2 (NO_2^-, m/e = 46) and HNO_3 ($F^-\cdot HNO_3$, m/e = 82). We are not aware of any measurements of the rate coefficient for reaction 3. The PNA concentration in the neutral flow reactor was estimated by assuming the same rate coefficient for reaction 3 as that for HNO_3 reaction with SF_6^- (∼2 × 10^{-9} molecules $cm^3\ s^{-1}$)[21] and by comparing the relative signal intensities between the two species under similar conditions (i.e., the same temperature, flow rate, and total pressure in the flow tube). This method requires accurate knowledge of the gas-phase partial pressure of HNO_3. The CIMS was calibrated for HNO_3 by measuring the flow rate of a known mixture of HNO_3 in He; the calibration procedure was described in detail in our previous work.[16,18] Alternatively, I^- ions, initiated by electron attachment to CF_3I, were used to detect HO_2NO_2 corresponding to NO_3^- (m/e = 62), as illustrated in

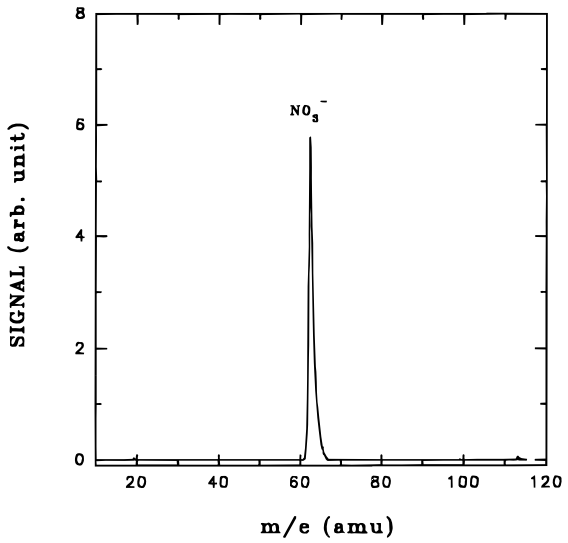

Figure 2. Mass spectrum of I^- reaction with the effluent from the PNA bubbler.

Figure 2:

$$I^- + HO_2NO_2 \rightarrow NO_3^- + HOI \qquad (4)$$

Reaction 4 also permits us to selectively probe PNA in the presence of HNO_3, because the reaction of I^- with HNO_3 is known to be rather inefficient.[21] Hence, HNO_3 impurity present in the PNA sample is unlikely to interfere with this detection scheme. Indeed, using SF_6^- or I^- as the reactant ions yielded no noticeable differences in the measurements of PNA uptake. To our knowledge, the rate coefficient for reaction 4 is also unknown. Note that in the present study accurate determination of the reactant concentrations was not required, although lower reactant concentrations were essential to minimize the occurrence of secondary reactions of potential product ions.

Ions were mass selected by a differentially pumped mass spectrometer and detected with a channeltron electron multiplier operated in an analogue mode. The CIMS detector was linear over the range of PNA concentrations used, since the concentration of the reactant ion was not affected by the small concentrations of the neutral reactant. Detection sensitivity of HO_2NO_2 in the CIMS was estimated to be $\sim 5 \times 10^7$ molecules cm^{-3} with a S/N ratio of unity for 1 s integration time.

In general, gas-phase uptake by a planar liquid surface is due to either time-dependent physical adsorption or irreversible chemical reaction, which can be treated by a diffusional and reactional equation.[22] The solution of time-dependent uptake with no chemical loss in a semiinfinite planar liquid has been given as[23]

$$\gamma_{obs}(t) = \alpha[1 - \mathrm{erf}\,(h\sqrt{t/D_l})]e^{h^2t/D_l} \qquad (5)$$

where $h = \alpha\omega/(4RTH^*)$, α is the mass accommodation coefficient, ω is the mean thermal speed of the molecule, R is the gas constant (0.082 L atm mol^{-1} K^{-1}) , T is the temperature, H^* is the effective Henry's law solubility constant, D_l is the liquid-phase diffusion coefficient, and erf(x) is the Gaussian error function. Under the condition that $h\sqrt{t/D_l} \gg 1$ (i.e., lower solubility or longer time), this solution can be approximated as[24]

$$\gamma_{obs}(t) \approx \frac{4RTH^*}{\omega}\left(\frac{D_l}{\pi t}\right)^{1/2} \qquad (6)$$

Hence, eq 6 relates the measured time-dependent uptake coefficient (γ_{obs}) to the product of the effective Henry's law solubility constant and the square root of the liquid-phase diffusion coefficient ($H^*\sqrt{D_l}$). Since the thickness of liquid sulfuric acid films (l) used in the present study was finite, eqs 5 and 6 apply only when $l \gg l_d$, where l_d ($l_d = (\pi D_l t)^{1/2}$) is the characteristic depth of liquid-phase diffusion at time t. As a result, some uptake data at sufficiently longer times (such that when l_d approached l) were not used in obtaining the PNA solubility. The uptake coefficient was calculated from the initial and time-dependent signals of PNA[25]

$$\gamma_{obs}(t) = \frac{2rk}{\omega + rk} \qquad (7)$$

where r is the radius of the flow reactor. The first-order rate coefficient (k) is related to the fractional change ($\Delta n/n$) in the gas-phase concentration of the adsorbed/reactive molecule (i.e., HO_2NO_2) before and after exposure to sulfuric acid by

$$k \approx \frac{2F_g}{rA}\left(\frac{\Delta n}{n}\right) \qquad (8)$$

where F_g is the carrier gas volume flow rate (cm^3 s^{-1}) and A is the surface area of exposed liquid. When the uptake rate became gas-phase diffusion limited, the first-order rate coefficient was corrected for gas-phase diffusion restrictions according to the method suggested by Brown.[26] The gas-phase diffusion coefficient of PNA in He was estimated to be $PD_g = 240$ Torr cm^2 s^{-1} at 220 K, with a temperature dependence of $T^{1.75}$.[27] These corrections were approximately 10% for smaller γ values ($\gamma < 0.01$), and as large as a factor of 4 for larger γ's ($\gamma > 0.2$).

To estimate the liquid-phase diffusion coefficient, we adopted a cubic cell model, which was initially developed for self-diffusion in liquids:[28,29]

$$D_l = \frac{RT\rho\lambda^2}{6\eta M_{PNA}} \qquad (9)$$

$$\lambda = \frac{1}{2}\left(d + \left[\frac{xM_{SO_4^{2-}} + (1-x)M_{H_2O}}{\rho}\right]^{1/3}\right) \qquad (10)$$

where ρ is the density of liquid H_2SO_4 and x is the H_2SO_4 mole fraction. M_{PNA}, $M_{SO_4^{2-}}$, and M_{H_2O} are the molecular weights of PNA, SO_4^{2-}, and, H_2O, respectively. Assuming that there is no liquid-phase dissociation, we estimated an effective molecular dimension (d) of $\sim$4 Å for PNA diffusing in liquid sulfuric acid, when calculating the parameter of the effective cell dimension (λ). The viscosity coefficient (η) of sulfuric acid, used in eq 9, incorporated the viscosity measurements by Williams and Long.[30] Table 1 lists some calculated values of the diffusion coefficient of PNA in sulfuric acid.

TABLE 1: Calculated Liquid-Phase Diffusion Coefficient D_l (in Units of 10^{-8} cm^2 s^{-1}) for PNA in Sulfuric Acid Based on the Cubic Cell Model

	wt %				
temp (K)	50	55	60	65	70
210	3.1	2.2	1.4	0.8	0.3
220	8.0	6.1	4.2	2.6	1.3
230	17.2	13.6	10.0	6.6	3.8

Results and Discussion

PNA Uptake Measurements. The uptake measurements were performed by first establishing a steady-state PNA flow, which bypassed the liquid film. The direction of the PNA flow was then quickly changed from downstream to upstream via

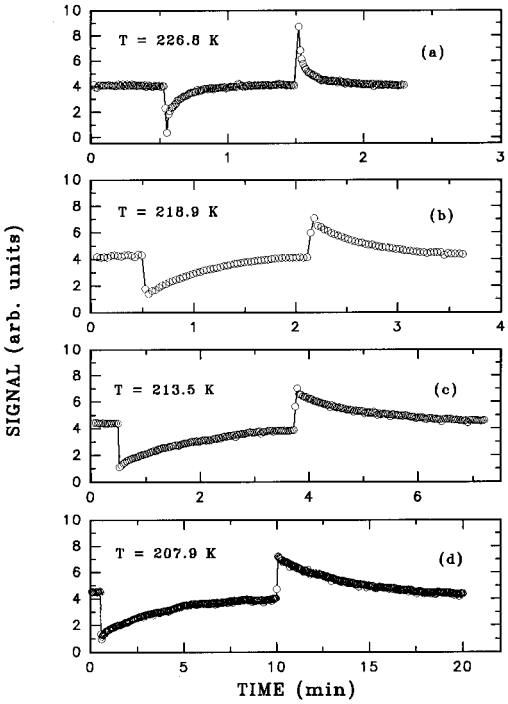

Figure 3. Temporal profiles of PNA when exposed to a 3.9-cm length of a sulfuric acid film at (a) 226.8, (b) 218.9, (c) 213.5, and (d) 207.9 K. The acid content of the film was estimated to be ~58.3 wt %. Experimental conditions are $P_{He} = 0.40$ Torr, $V \approx 1900$ cm s^{-1}, and $P_{PNA} \approx 5 \times 10^{-7}$ Torr.

the three-way switching valve, exposing a 3−5 cm length of the film to PNA, while monitoring the PNA signal using the CIMS. Uptake from the gas phase was determined from the decline and recovery in the PNA signal. Figure 3 shows temporal profiles of PNA as it was exposed and not exposed to a 3.9 cm length of a liquid sulfuric acid film at 207.9, 213.5, 218.9, and 226.8 K, respectively. The liquid film was initially allowed to equilibrate with H_2O vapor at a partial pressure of 6.9×10^{-4} Torr and at 207.9 K; the acid content of the film was estimated to be ~58.3 wt %. The temperature of the flow tube was quickly raised and then held steady at a higher value to carry out the next measurement. The experimental conditions corresponding to these measurements were $P_{He} = 0.40$ Torr, $V \approx 1900$ cm s^{-1}, and $P_{PNA} \approx 5 \times 10^{-7}$ Torr. Even though water vapor was continuously added to the system at $P_{H_2O} = 6.9 \times 10^{-4}$ Torr during the warming process (typically less than 20 min), evaporation of H_2O at higher temperatures may cause some change in the film composition. We estimated that in the section of the acid film used in the uptake measurements (i.e., 3−5 cm downstream of the flow reactor) the composition change would be less than 2 wt %, based on parallel observations in which the H_2O signal was continuously monitored using an electron-impact ionization mass spectrometer for liquid films under similar conditions (i.e., the same temperatures, flow rates, total pressures, and time scales), as described in our previous publication.[16] In addition, these measured Henry's law solubility constants did not differ significantly from those measured when the film was considered to be in equilibrium with water vapor, to be discussed below.

Figure 3 shows that the PNA concentration in the gas phase fell instantly upon exposure to H_2SO_4 and later returned to its original value as the film was saturated. Switching the PNA flow downstream resulted in an opposite peak due to desorption. The shapes of adsorption and desorption processes were nearly identical, suggesting that PNA was physically taken up by liquid sulfuric acid without undergoing irreversible aqueous-phase reactions. This held true over the entire H_2SO_4 content and temperature ranges investigated, i.e., over H_2SO_4 contents of 53−74 wt % and temperatures of 205−230 K. As can be seen from Figure 3, the amount of PNA taken up by the liquid film increased as the temperature decreased. This occurred because solubility of PNA increased with decreasing temperature (see discussion below). Under no circumstances did we observe any gaseous products by the CIMS associated with PNA uptake in sulfuric acid. In particular, we found no evidence for the occurrence of reaction 2 in liquid sulfuric acid (HONO can be detected using SF_6^- corresponding to $F^-\cdot$HONO at $m/e = 66$)[31].

To test whether reaction 2 proceeds slowly in sulfuric acid, as was the case suggested in aqueous O_2-saturated nitrate solutions,[10] we exposed PNA continuously to sulfuric acid over a time period of more than 3 h and then identified the constituents in the liquid phase, using a temperature-programmed desorption method. Two measurements were carried out for liquid films of 50 and 70 wt % and at temperatures of 201 and 222 K, respectively. No reaction products other than PNA were observed in these experiments. Also, the NO_2 impurity present in the PNA sample was too small to produce any appreciable amount of nitrous acid by the reaction of NO_2 with H_2O. This reaction, however, may occur if very high NO_2 concentrations are present, and it may explain the observation of HONO production in the environmental chamber experiment reported by Zhu et al.,[11] likely with NO_2 derived from thermal decomposition of PNA. As reported in a separate publication by us,[31] HONO undergoes complex aqueous phase reactions in liquid sulfuric acid, depending on the acidity.

Determination of $H^*\sqrt{D_l}$ and H^*. Uptake of PNA into sulfuric acid may take place in several steps, including solvation, dissociation, and ionic reactions with the constituents in the liquid:[10]

$$HO_2NO_2(g) \rightleftharpoons HO_2NO_2(aq) \tag{11}$$

$$HO_2NO_2 \rightleftharpoons H^+ + O_2NO_2^- \tag{12}$$

$$O_2NO_2^- \rightarrow NO_2^- + O_2 \tag{13}$$

The acid equilibrium constant of PNA in aqueous nitrite solutions was determined to be 1.4×10^{-6} at room temperature,[10] indicating that PNA is a relatively weak acid. Under stratospheric conditions, reaction 13, along with reaction 2 and unimolecular decomposition of PNA into HO_2 and NO_2, can be ignored in sulfuric acid, as concluded in the preceding section. An effective Henry's law solubility constant that encompasses the totality of the dissolved species is defined as[32]

$$H^* = H\{1 + k_{12}/[H^+]\} \tag{14}$$

$$[HO_2NO_2(\text{total})] = [HO_2NO_2(aq)] + [O_2NO_2^-] = P_{PNA}H^* \tag{15}$$

where H is the physical Henry's law solubility constant (i.e., the equilibrium constant for reaction 11).

For the data displayed in Figure 3, the time-dependent uptake coefficients were calculated from the initial and time-dependent PNA signals using eq 7. Figure 4 shows a plot of $\gamma_{obs}(t)$ as a function of time. The uptake coefficient is initially very large (about a few tenths) and then decreases rapidly with time, indicating that at longer times the decreasing uptake coefficient is a manifestation of both solubility and liquid-phase diffusion

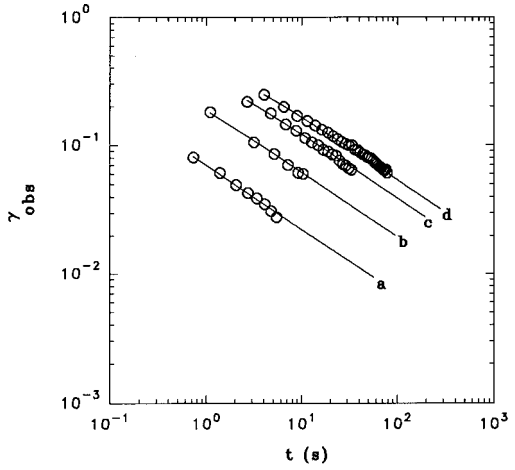

Figure 4. Uptake coefficients of PNA on liquid sulfuric acid as a function of time for data displayed in Figure 3. The solid curves are obtained on the basis of a numerical solution to eq 5. A value of $H^*\sqrt{D_l}$ is determined from the best fit of the data.

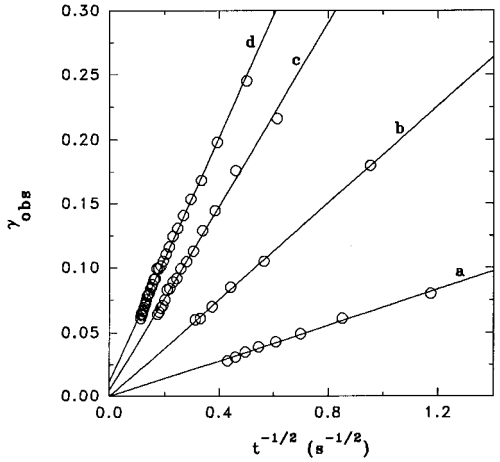

Figure 5. Similar to Figure 4 except for the uptake coefficient as a function of $t^{-1/2}$ based on eq 6. The lines through the data are linear least-squares fits.

limitations.[33] Shown as the solid curves in Figure 4 are fittings of the data using eq 5, based on a numerical solution to the Gaussian error function. The values of $H^*\sqrt{D_l}$ corresponding to curves a−d in Figure 4 are 42.4, 114.8, 213.5, and 324.9 M atm^{-1} cm s^{-1}, respectively. We have taken unity for the mass accommodation coefficient (α) while using eq 5. Note that some longer time data were not used in the analysis, since the characteristic depth (l_d) of liquid-phase diffusion may approach the film thickness at larger t and eq 5 no longer applies; as discussed above, l_d is determined by both temperature and acid composition. The same data shown in Figure 4 are also given in Figure 5 as a plot of $\gamma_{obs}(t)$ versus $t^{-1/2}$. The solid curves are linear least-squares fittings through the data, in accordance with eq 6. Since the quantity $h\sqrt{t/D_l}$ is much greater than one (except for $t < 1$ s), the conditions for eq 6 to be valid are also satisfied. The slopes of the lines are proportional to $H^*\sqrt{D_l}$, yielding 40.8, 112.5, 216.1, and 291.1 M atm^{-1} cm s$^{-1/2}$ for this parameter at 226.8, 218.9, 213.5, and 207.9 K, respectively. Hence, using eqs 5 and 6 results in a difference of less than 15% in the values of $H^*\sqrt{D_l}$ obtained in the present study. Some of the differences may be associated with the limitation in accurately obtaining the uptake coefficient, $\gamma_{obs}(t)$, when its value is larger than 0.1, because there is a large uncertainty linked to the correction of the gas-phase diffusion under this condition.

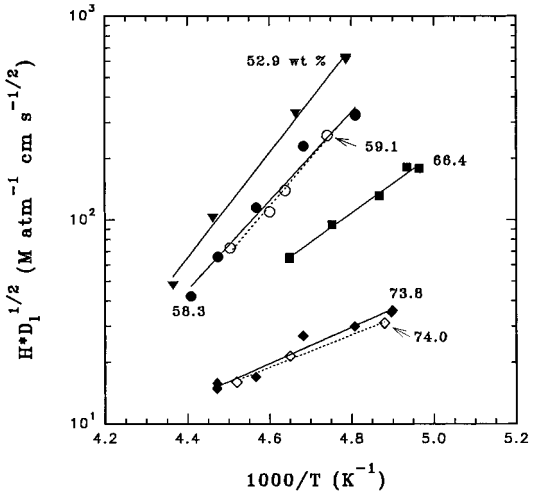

Figure 6. Measured values of $H^*\sqrt{D_l}$ against the reciprocal of temperature for various H_2SO_4 contents. The solid lines are linear fits through the data. The open symbols are measurements using liquid films prepared by coating two known acid compositions. Experimental conditions are $P_{He} = 0.40$ Torr, $V = 1700-2000$ cm s^{-1}, and $P_{PNA} \approx 5 \times 10^{-7}$ Torr.

Measured values of $H^*\sqrt{D_l}$ for PNA in sulfuric acid of various concentrations are shown against the reciprocal of temperature in Figure 6. The solid symbols were data obtained by first establishing an equilibrium sulfuric acid film (typically a few hours) at a given H_2O partial pressure and temperature. The temperature of the substrate was then successively raised while the uptake data were taken (examples of the uptake and desorption data have been given in Figure 3). Also shown in Figure 6 as open symbols are two measurements using liquid films prepared by coating two known acid compositions of 59.1 and 74.0 wt %, respectively. For these two cases, water vapor in the flow reactor was regulated to compensate for possible changes in the acid content. Clearly, there are no systematic differences in the measured quantity $H^*\sqrt{D_l}$, using the two different approaches in obtaining the acid compositions. Figure 6 shows that the quantity $H^*\sqrt{D_l}$ increases both as the temperature is lowered and as the solution becomes more dilute. This is expected since physical solubility in general increases with decreasing temperature and decreasing acid content. Additionally, it is also plausible that the extent of PNA dissociation may enhance slightly at lower temperatures, leading to larger values of the effective Henry's law constants. Uncertainty in $H^*\sqrt{D_l}$ values is about 15% for smaller $H^*\sqrt{D_l}$ values (< 100 M atm^{-1} cm s$^{-1/2}$) and may be as large as 40% for larger $H^*\sqrt{D_l}$ (>500 M atm^{-1} cm s$^{-1/2}$), due to the uncertainty in the measurements of γ_{obs}. Measurements of the quantity $H^*\sqrt{D_l}$ for PNA in various sulfuric acid solutions are also listed in Table 2.

In another set of experiments, PNA uptake was studied by maintaining a constant H_2O partial pressure and by varying temperature and allowing water vapor to equilibrate with the liquid (typically a few hours). This is a process resembling the compositional change of sulfate aerosols during a cooling or warming event in the stratosphere. The results are consistent with those displayed in Figure 6.

Effective Henry's constants were derived by estimating the liquid-phase diffusion coefficient of PNA in sulfuric acid. H^* corresponding to data in Figure 6 are given in Figure 7. The slopes of the lines in the figure represent the enthalpy difference of PNA in the solution and in the gas phase, which are correlated to the enthalpy changes of reactions 11 and 12. Figure 7 shows that the solubility constants in various H_2SO_4 solutions have

TABLE 2: Measured Values of $H^*\sqrt{D_l}$ for HO_2NO_2 in H_2SO_4

H_2SO_4 (wt %)	temp (K)	$H^*\sqrt{D_l}$ (M atm^{-1} cm s$^{-1/2}$)	H^* (M atm^{-1})
52.9[a]	208.9	616.6	3.9×10^6
	208.9	632.5	4.0×10^6
	214.4	337.9	1.6×10^6
	224.1	103.2	3.2×10^5
	229.1	48.3	1.7×10^5
58.3[a]	207.9	330.7	2.9×10^6
	207.9	324.9	2.9×10^6
	213.5	203.1	1.4×10^6
	218.9	114.8	5.5×10^5
	223.5	66.0	2.5×10^5
	226.8	42.4	1.5×10^5
66.4[a]	201.4	178.8	5.0×10^6
	202.6	181.6	4.5×10^6
	205.4	131.5	2.5×10^6
	210.4	94.8	1.2×10^6
	215.1	65.7	6.0×10^5
	215.1	64.6	5.9×10^5
73.8[a]	204.1	36.1	2.6×10^6
	204.2	35.2	2.5×10^6
	208.0	30.0	1.3×10^6
	213.6	26.8	6.3×10^5
	219.0	17.2	2.5×10^5
	223.6	15.3	1.6×10^5
	223.6	15.8	1.6×10^5
	223.6	14.8	1.5×10^5
59.1[b]	210.9	260.4	1.9×10^6
	215.6	139.8	7.9×10^5
	217.4	110.5	5.7×10^5
	222.0	73.2	3.0×10^5
74.0[b]	204.9	31.2	2.1×10^6
	215.1	21.5	4.5×10^5
	221.2	16.1	2.0×10^5

[a] Estimated from the temperature and water partial pressure. [b] Obtained from the density measurements.

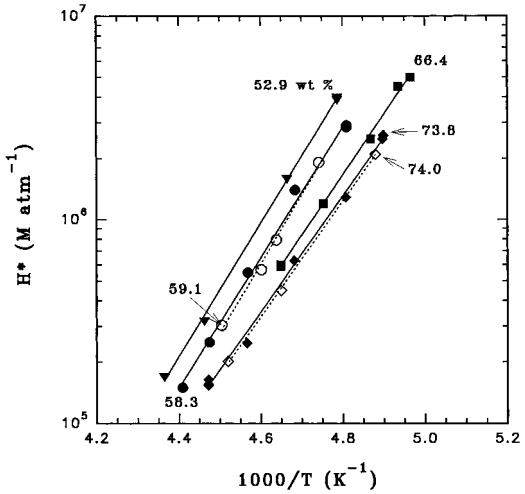

Figure 7. Same as Figure 6 except for H^* calculated by estimating the liquid-phase diffusion coefficient using the cubic cell model.

similar temperature dependencies, indicating a nearly constant activity coefficient over the temperature range. For a given acid composition, the temperature dependence of the effective Henry's law constant is expressed by $\ln H^* = -\Delta H/RT + \Delta S/R$, where ΔH and ΔS are the changes of enthalpy and entropy associated with the PNA solvation. The values of ΔH derived from the present study vary from -15.0 to -13.0 kcal mol^{-1}, in the acid content range 52.9−74.0 wt %; the change in entropy, ΔS, also varies from -41.6 to -34.4 cal mol^{-1} K^{-1} in the same acid composition range. It is seen from the figure that H^* depends strongly on temperature but rather weakly on acid content. This may be expected since PNA is a relatively weak acid, and its dissociation over the acid composition range is expected to be small. This is in contrast to other acid species such as HCl and HNO_3: the extents of their acid−base dissociations in sulfuric acid increase rapidly with decreasing sulfuric acid content at a given temperature[34−36] and, accordingly, the effective Henry's law constants increase markedly with decreasing sulfuric acid content. Our observations of a weak dependence of the PNA effective Henry's law constant on the H_2SO_4 acidity are similar to those of HOCl in sulfuric acid reported previously.[37] The uncertainty associated with the Henry's law constant was estimated to be about 25% for H^* less than 1×10^6 M atm^{-1} and 50% for H^* larger than 1×10^6 M atm^{-1}, considering the uncertainties related to the composition and viscosity of sulfuric acid.

The uptake measurements reported here were restricted to temperatures above 205 K. Below this temperature, the time to saturate the liquid film became so long that the PNA source became unstable. Also, at low temperatures and in dilute sulfuric acid, the Henry's law may not be a valid description of the solubility behavior, because of the departure from ideality or increasing activity coefficient.[36] Solubility of PNA in liquid sulfuric acid, as determined in the present study, is fairly large: under identical conditions (i.e., the same H_2SO_4 content and temperature) the effective Henry's law constant for PNA is smaller than that of HNO_3,[34] but larger than that of HCl.[24,36] Hence, it would be worthwhile to examine some potential heterogeneous reactions involving PNA on sulfuric acid.

Reaction of HO_2NO_2 with HCl. The gas-phase reaction between HO_2NO_2 and HCl has been found to be very slow, with a rate constant of less than 9×10^{-22} cm^3 s^{-1}:[38]

$$HO_2NO_2 + HCl \rightarrow HOCl + HNO_3 \qquad (16)$$

This reaction, if proceeding in bulk sulfuric acid solutions, will likely produce gaseous Cl_2 or HOCl, dependent on the relative concentrations of HCl and PNA.[16,39] This situation arises because the secondary reaction between the product HOCl and HCl will take place in the solution to form Cl_2. The experiments were carried out by first allowing the H_2SO_4 film to equilibrate with HCl (or HO_2NO_2) introduced from the gas phase and then measuring the HO_2NO_2 (or HCl) uptake. Partial pressures of PNA and HCl were maintained in the range 10^{-6}−10^{-7} Torr. For acid contents of 50−70 wt % and temperatures of 201−222 K, we did not observe any measurable reaction between PNA and HCl nor any possible reaction products (Cl_2 or HOCl). In the CIMS, Cl_2 and HOCl can be detected as Cl_2^- and ClO^- using SF_6^- and F^-, respectively. A conservative upper limit of 1×10^{-4} for this reaction probability was estimated on the basis of our experimental conditions. Thus, we conclude that reaction 16 is of negligible importance on stratospheric sulfate aerosols.

Stratospheric Implications. Using our determined effective Henry's law solubility constants, equilibrium concentrations of PNA in sulfate aerosols can be estimated. For a nominal 55 wt % sulfate aerosol at 205 K, the value of H^* is found to be $\sim 6 \times 10^6$ M atm^{-1} according to Figure 7. This results in an equilibrium PNA concentration of about 10^{-4} M for a typical PNA mixing ratio of 0.1 ppbv at 100 mb (i.e., a partial pressure of 10^{-8} Torr). At temperatures below 205 K, this equilibrium concentration should increase significantly, as indicated in Figure 7. Nevertheless, we believe that PNA is unlikely a major component of stratospheric aerosols, even when the temperature is below 200 K, since PNA solubility is about 2 orders of magnitude smaller than that of HNO_3 and also the stratospheric PNA concentration is an order of magnitude smaller than that of HNO_3.

The distribution of PNA between the gas and condensed phases can be estimated by,

$$[HO_2NO_2(\text{aerosol})]/[HO_2NO_2(g)] = P_{PNA}H^*L/(P_{PNA}/RT) = H^*LRT \quad (17)$$

where L is the volume fraction of the condensed phase in air. Using L values of 10^{-14} and 10^{-10} corresponding to "background" and "volcanically perturbed" aerosol conditions,[40] the ratios are $\sim 1.2 \times 10^{-6}$ and $\sim 1.2 \times 10^{-2}$ at 205 K, respectively. In the middle or lower latitude stratosphere, where the ambient temperature is higher than 210 K, PNA should exist exclusively in the gas phase. Using an extrapolated value of $\sim 2 \times 10^8$ M atm^{-1} for H^* at 190 K and a L value of 10^{-10} for supercooled aerosols under elevated sulfate aerosol loading conditions,[40,41] this ratio can reach about 30% in the winter polar stratosphere. Hence, at these conditions incorporation of PNA into the supercooled aerosols may lead to redistribution of PNA from the gas to condensed phase, which may affect stratospheric NO_x and HO_x concentrations.

Finally, the characteristic time for stratospheric sulfate aerosols to reach equilibrium is estimated by[32]

$$t = (2H^*RTd)/(3\alpha\omega) \quad (18)$$

Using a mean particle diameter of 0.1 μm and an accommodation coefficient of unity, the characteristic time is about 0.1 s, suggesting that equilibrium between the gas and condensed phases is constantly maintained.

Conclusions

In this paper we have reported laboratory measurements of interaction of PNA vapor with liquid sulfuric acid. PNA was observed to be physically taken up by sulfuric acid, without undergoing irreversible chemical reactions. The uptake data show that PNA is very soluble in liquid sulfuric acid: the solubility was found to increase with decreasing acid content and decreasing temperature. In middle or lower latitude stratosphere, PNA should exist primarily in the gas phase. In very cold stratospheric regions and under elevated sulfate aerosol loading conditions, uptake of PNA by sulfate aerosols could reduce gaseous PNA concentrations, possibly affecting the HO_x and NO_x budgets. Heterogeneous reaction between PNA and HCl was concluded to be unimportant on sulfate aerosols in the stratosphere.

Acknowledgment. The research was performed at the Jet Propulsion Laboratory, California Institute of Technology, under a contract with the National Aeronautics and Space Administration (NASA). We thank Z. Li, R. R. Friedl, and S. P. Sander for helpful discussions.

References and Notes

(1) DeMore, W. B.; Sander, S. P.; Howard, C. J.; Ravishankara, A. R.; Golden, D. M.; Kolb, C. E.; Hampson, R. F.; Kurylo, M. J.; Molina, M. J. *Chemical Kinetics and Photochemical Data for Use in Stratospheric Modeling*; JPL Publication 94-26, NASA, 1994.

(2) Kolb, C. E.; Worsnop, D. R.; Zahniser, M. S.; Davidovits, P.; Hanson, D. R.; Ravishankara, A. R; Keyser, L. F.; Leu, M. T.; Williams, L. R.; Molina, M. J.; Tolbert, M. A. In *Current Problems in Atmospheric Chemistry*; Barker, J. R., Ed.; *Adv. Phys. Chem.*; World Scientific Publishing: New York, 1995.

(3) Turco, R. P.; Whitten, R. C.; Toon, O. B. *Rev. Geophys.* **1982**, *20*, 233.

(4) Niki, H.; Maker, P. D.; Savage, C. M.; Breitenback, L. P. *Chem. Phys. Lett.* **1977**, *45*, 564.

(5) Howard, C. J. *J. Phys. Chem.* **1977**, *67*, 5258.

(6) Brasseur, G.; Solomon, S. *Aeronomy of the Middle Atmosphere*; D. Reidel Publishing Co.: Boston, 1984.

(7) Yung, Y. L., private communication, 1995.

(8) Macleod, H.; Smith, G. P.; Golden, D. M. *J. Geophys. Res.* **1988**, *93*, 3813.

(9) Kenley, R. A.; Trevor, P. L.; Lan, B. Y. *J. Am. Chem. Soc.* **1981**, *103*, 2203.

(10) Logager, T.; Sehested, K. *J. Phys. Chem.* **1993**, *97*, 10047.

(11) Zhu, T.; Yarwood, G.; Chen, J.; Niki, H. *Environ. Sci. Technol.* **1993**, *27*, 982.

(12) Salawitch, R. J.; et al. *Geophys. Res. Lett.* **1994**, *23*, 2551.

(13) Wennberg, P. O.; et al. *Science*, **1994**, *266*, 398.

(14) Li, Z.; Friedl, R. R.; Sander, S. P. *J. Geophys. Res.* **1996**, *101*, 6795.

(15) Baldwin, A. C.; Golden, D. M. *J. Geophys. Res.* **1980**, *85*, 2888.

(16) Zhang, R.; Leu, M. T.; Keyser, L. F. *J. Phys. Chem.* **1994**, *98*, 13563.

(17) Leu, M. T.; Timonen, R. S.; Keyser, L. F.; Yung, Y. L. *J. Phys. Chem.* **1995**, *99*, 13203.

(18) Zhang, R.; Leu, M. T.; Keyser, L. F. *J. Geophys. Res.* **1995**, *100*, 18845.

(19) Zeleznik, F. J. *J. Phys. Chem. Ref. Data* **1991**, *20*, 1157.

(20) Zhang, R.; Wooldridge, P. J.; Abbatt, J. P. D.; Molina, M. J. *J. Phys. Chem.* **1993**, *97*, 7351.

(21) Huey, L. G.; Hanson, D. R.; Howard, C. J. *J. Phys. Chem.* **1995**, *99*, 5001.

(22) Danckwerts, P. V. *Gas-Liquid Reactions*; McGraw-Hall: New York, 1970.

(23) Danckwerts, P. V. *Trans. Faraday Soc.* **1951**, *47*, 1014.

(24) Hanson, D. R.; Ravishankara, A. R. *J. Phys. Chem.* **1993**, *97*, 12309.

(25) Motz, H.; Wise, H. *J. Chem. Phys.* **1960**, *32*, 1893.

(26) Brown, R. L. *J. Res. Natl. Bur. Stand. (U.S.)* **1978**, *83*, 1.

(27) Marrero, T. R; Mason, E. A. *J. Phys. Chem. Ref. Data*, **1972**, *1*, 3.

(28) Houghton, G. *J. Chem. Phys.* **1964**, *40*, 1628.

(29) Luo, B. P.; Clegg, S. L.; Peter, T.; Muller, R.; Crutzen, P. J. *Geophys. Res. Lett.* **1994**, *21*, 49.

(30) Williams, L. R.; Long, F. S. *J. Phys. Chem.* **1995**, *99*, 3748.

(31) Zhang, R.; Leu, M. T.; Keyser, L. F. *J. Phys. Chem.* **1996**, *100*, 339.

(32) Schwartz, S. E. In *Chemistry of Multiphase Atmospheric Systems*; Jaeschke, W., Ed.; NATO ASI Series, Vol. G6; NATO: Brussels, 1986.

(33) Worsnop, D. R.; Zahniser, M. S.; Kolb, C. E.; Gardner, J. A.; Watson, L. R.; Van Doren, J. M.; Davidovits, P. *J. Phys. Chem.* **1989**, *93*, 1159.

(34) Sampoli, M.; De Santis, A.; Marziano, N. C.; Pinna, F.; Zingales, A. *J. Phys. Chem.* **1985**, *89*, 2864.

(35) Watson, L. R.; Van Doren, J. M.; Davidovits, P.; Worsnop, D. R.; Zahniser, M. S.; Kolb, C. E. *J. Geophys. Res.* **1990**, *95*, 5631.

(36) Zhang, R.; Wooldridge, P. J.; Molina, M. J. *J. Phys. Chem.* **1993**, *97*, 8541.

(37) Huthwelker, T; Peter, Th.; Luo, B. P.; Clegg, S. L.; Carslaw, K. S.; Brimblecombe, P. *J. Atmos. Chem.* **1995**, *21*, 81.

(38) Leu, M. T.; Hatakeyama, S.; Hsu, K. J. *J. Phys. Chem.* **1989**, *93*, 5778.

(39) Hanson, D. R.; Ravishankara, A. R. *J. Phys. Chem.* **1994**, *98*, 5728.

(40) Hofmann, D. J.; Oltmans, S. J.; Solomon, S.; Deshler, T.; Johnson, B. J. *Nature* **1992**, *359*, 183.

(41) Dye, J. E.; et al. *J. Geophys. Res.* **1992**, *97*, 8015.